31st Congress of the International Council of the Aeronautical Sciences

Belo Horizonte, Brazil; September 09-14, 2018

INFLUENCE OF GULL WING ON LONGITUDINAL AND LATERAL-DIRECTIONAL COEFFICIENTS OF AN AIRPLANE

Atila A. F. Barbosa*, Fernando M. Catalano*
***University of Sao Paulo (EESC-USP), Sao Carlos, Sao Paulo, 13566-590**

Keywords: *gull wing, multi-dihedral wing, wind tunnel testing*

Abstract

In the beginning of the 2010s, the increasing price of aviation fuel and the pressure of society to reduce the emission of harmful gases into the environment, coupled with the need of noise reduction during the takeoff and landing, induce carrier companies to look for more efficient airplanes. To furnish this demand, the airplane manufacturers solved the problem using high performance engines, which present a larger diameter than the engines from previous generations. Thereby, it was necessary to project wing with higher dihedral on the root portion, enabling the installation of these new engines, and a lower dihedral after the engine section, thus adopting a gull wing solution. This article aims at analyzing the impact of different types of gull wing on lift, drag and pitch moment coefficients (longitudinal) and yawing moment coefficient (lateral-directional) of a typical commercial configuration airplane. For this purpose, a bibliographic review about the studies related to gull wings was performed. In a first phase, an analytical analysis of the aerodynamic coefficients some airplane model with gull wings was done, and in a second phase, computational programs were used to study their aerodynamic behavior. Later, in a third phase, these models were tested in wind tunnel and the results from the three phases were compared.

1 Introduction

The choice of the wing dihedral angle during the preliminary design phase must be based on the balance between lateral stability and Dutch roll stability. The geometric ground clearance is also a deciding factor, according to [1]. The airplane manufacturers solved this trade between stability and ground clearance by using gull wing configuration, when they had to install the high by-pass engines under their airplane wings. The high by-pass engines were developed as a solution to the demand from carrier companies to a more efficient engine, caused by the high aviation fuel prices, and the need of harmful gases and noise reduction.

In addition to the new engines the composite materials allowed the airplane manufacturers to increase the wing aspect ratio of the airplanes, by enlarging its wing span, aiming at reducing fuel consumption. When the wing aspect ratio is augmented, there is a reduction of induced drag. However, higher aspect ratio increases the wing bending; for instance, the wingtips from Boeing 787 Dreamliner displace almost 3 m under normal flight loads and approximately 8 m under ultimate loads [2]. This wing bending is not uniform along the wing span due to the stiffer structure near the wing root and the engine weight, and alters the wing dihedral unevenly, in a configuration that can be approximated by a gull wing.

Early studies about the gull wing date back from 1938, when it was observed that the estimation of rolling moment coefficient due to sideslip angle could be performed considering separately the influence of each dihedral angle along the wing span [3].

In 1946, Ankelbruck [4] performed tests considering an inverted gull wing, and concluded that this configuration promoted abnormal lateral oscillations at high lift coefficients, caused by reduction the damping in roll due to the early stalling at the dihedral

break. No effects were observed for the lower lift coefficients.

More recently (2004), Abdulharim [5] noted experimentally that wings with constant dihedral along span presented a better glide ratio when compared to normal and inverted gull wings. Additionally, gull wing configuration presented an increase in lateral stability and inverted gull wing configuration showed a reduction in lateral stability and contributed to a more aggressive stall mode.

2 Methodology

To evaluate the characteristics of gull wings in longitudinal and lateral-directional coefficients, standard comercial airplane geometry was chosen and three different types of analysis were performed, as detailed in the following chapters.

2.1 Geometry Description

The airfoil selection was driven by the characteristics of the closed wind tunnel test section available in the Laboratory of Aerodynamics (LAE) from the University of Sao Paulo (EESC-USP), that are presented in Tab. 1. Due to the width of the test section, the model wing span was defined as 1.2 m.

Tab. 1. Wind tunnel test section characteristics

Height	1.3 m
Width	1.7 m
Length	3.0 m
Max operational speed	45 m/s

In addition, considering that flow speed during the tests would be around 25 m/s, the Reynolds number based on the model chord was close to 200,000. Another criterion for the airfoil selection was lift coefficient (C_L) for angle of attack (α) equal to 0.50, which is typical for commercial airplanes. Taking into account all the considerations stated before, the Clark-Y airfoil was selected. Furthermore, Selig, Donovan and Fraser [6] observed that for Clark-Y airfoil, the separation of laminar flow only occurs when Reynolds number for the airfoil is lower than 100,000.

One interesting characteristic of Clark-Y airfoil is that its lower surface is flat from 30% of chord, making simpler angle measurements, and its maximum thickness is 11.72%, making possible the hinge components to be installed inside the airfoil.

The wing planform, similar to conventional commercial jets, and the front view are presented in Fig. 1. The relevant geometric parameters are shown in Tab. 2.

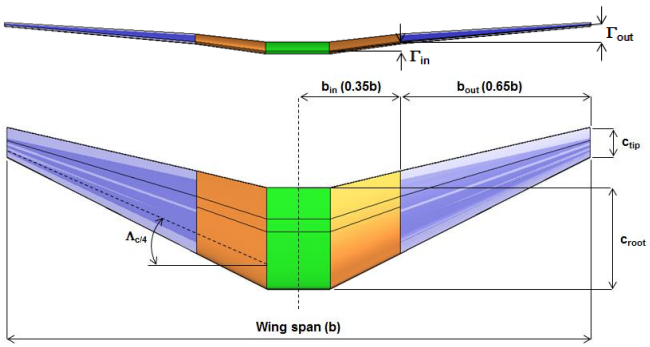

Fig. 1. Wing geometry – front and planform views

Tab. 2. Wing geometry

Wing span (b)	1.20 m
Wing reference area (S_{ref})	0.17 m^2
Aspect ratio (A)	8.40
Wing sweep at ¼ chord ($\Lambda_{c/4}$)	26.7 deg
Wing root chord (c_{root})	0.255 m
Wing reference chord (c_{ref})	0.160 m
Wing tip chord (c_{tip})	0.061 m
Taper ratio (λ)	0.29

Two hinges were installed on the wing: one at the root section and another at 35% from wing span (Fig. 1). Using these hinges, it was possible to combined different configurations of dihedral angles. The inboard and outboard dihedral selected angles are presented on Tab. 3. The values from Tab. 3 were specified taken into account data from current commercial airplanes and produced the nine different gull wing configurations studied in this paper.

Tab. 3. Values of wing dihedral [degrees]

Section	Low angle	Medium angle	High angle
Inboard (Γ_{in})	5.0	8.0	11.0
Outboard (Γ_{out})	2.0	5.0	8.0

2.2 Analytical Analysis

Analytical analysis was performed using classical lift and pitching moment slope estimation. Although, these methods do not consider the dihedral effect, they were selected to validate the results obtained using the other types of analysis.

The analytical analysis was not used for drag coefficient (C_D) and yawing moment coefficient estimation.

According to [1], the C_L versus α slope can be calculated using Eq. (1).

$$C_{L_\alpha} = \frac{2\pi A}{2 + \sqrt{\frac{A^2\beta^2\left[1 + \frac{\tan^2(\Lambda_{c/2})}{\beta^2}\right]}{k^2} + 4}} \quad (1)$$

Where β can be calculated using Eq. (2), k can be calculated using Eq. (3) and $\Lambda_{c/2}$ is the sweep angle measured in half-chord position.

$$\beta = (1 - M^2)^{1/2} \quad (2)$$

$$k = \frac{cl_\alpha \beta}{2\pi} \quad (3)$$

Where M is the Mach number and cl_α is the C_L versus α slope for the Clark-Y airfoil. This information was obtained from reference [6].

The pitching moment coefficient (C_m) versus α slope was calculated using the formulation proposed by [1] and is detailed in Eq. (4) and Eq. (5).

$$C_{m_\alpha} = \left(\frac{dC_m}{dC_L}\right)_w C_{L_\alpha} \quad (4)$$

$$\left(\frac{dC_m}{dC_L}\right)_w = \frac{(n_{ref} - n_{ac})}{\bar{c}} \quad (5)$$

Where n_{ref} is the reference point to pitching moment calculation, n_{ac} is the position of the aerodynamic center (both parameters measured from the wing apex) and $\bar{c}$ is the mean aerodynamic chord.

2.3 Computational Analysis

Computational analysis was performed using Tornado, version 135, software developed by Tomas Melin, as part of his master thesis [7] in the Royal Institute of Technology (KTH), Sweden. This program is based on the vortex lattice classical theory, derived from the potential flow theory. Due to the formulation, Tornado must be used only when the aerodynamics is linear, the angles attack and sideslip are small and the velocity is not high (compressibility effects are negligible). Another software was used to carry out the computational analysis, XFLR5, version 06.10.03. The Panels Method module was employed, without considering viscous effects.

The Tornado analyses were performed considering flow velocity equal to 25 m/s. For each wing section (center, inboard and outboard – see Fig. 1), a 10 panels chord-wise and span-wise discretization was used (100 panels). This grid selection was based on a previous mesh study presented in [8]. The same configuration was used in XFLR5. An example of mesh used in computational analysis is presented in Fig. 2.

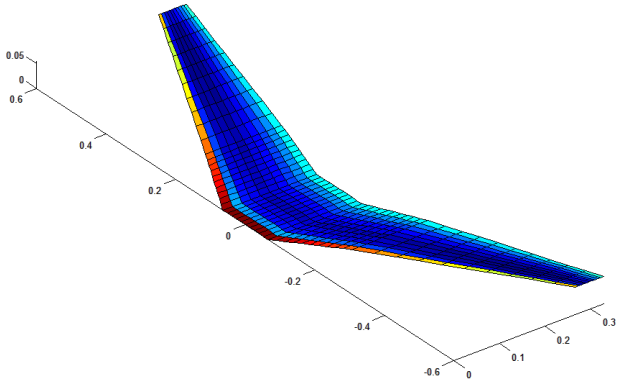

Fig. 2. Example of mesh distribution

Both longitudinal and lateral-directional analyses were performed considering angle of attack and angle of sideslip variations from -5 degree to +5 degree, for each of the nine possible dihedral combinations, using the inboard and outboard angles from Tab. 2.

2.4 Experimental Analysis

Experimental analysis for the longitudinal coefficients was performed using only half wing model. The open section wind tunnel from LAE EESC-USP was utilized, and the results were calculated directly from a 3 components balance, responsible for lift and drag forces and pitching moment measurements. This wind tunnel presents a test section of 1 m x 1.1 m,

and it contains a BSD BerlinerLuft centrifuge fan, which can accelerate the airflow up to 28 m/s in the test section, equivalent to a Reynolds number of 250,000 using the wing model chord as reference.

All longitudinal data were corrected using the method proposed by reference [9], which divides the wind tunnel corrections in two types: lift interference and blockage interference. Both corrections were applied in longitudinal data

For yawing moment coefficient, the full wing model was employed. The tests were performed in the closed section wind tunnel from LAE EESC-USP, previously detailed, and yawing moment due to yaw rate derivative was obtained using Free Oscillation Method, described in reference [10].

To apply the Free Oscillation Method, it was necessary to use a special measurement setup, illustrated in Fig. 3. In this setup, a direct current 5 volts source was connected to an oscilloscope, and it was linked to a potentiometer.

The potentiometer was connected to a horizontal shaft, where the wing was attached through a vertical shaft. Two springs of pre-defined stiffness were also connected to the horizontal shaft.

Only the vertical shaft and the wing from Fig. 3 were positioned inside the wind tunnel test section. All the other equipments were installed below the test section and could be accessed any moment during the experiment.

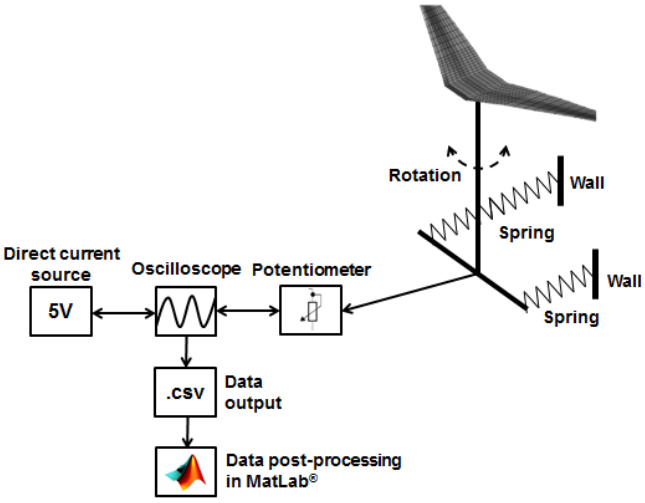

Fig. 3. Measurement setup used for the oscillatory test

When the gull wing was rotated, a difference of tension was caused by the movement of the potentiometer. This tension variation was captured by the oscilloscope and it was directly saved in .csv (Comma Separated Values) files.

For each dihedral configuration tested, an output file using a sampling rate of 1250 Hz was saved. The .csv files were formed by 62500 points, divided in two columns, tension and time. In the sequence, these data were filtered and the number of points reduced to approximately 2500 in each file.

Using the filtered data, the method described in reference [10] was applied, and the yawing moment due to yaw rate derivative was calculated.

To modify the inboard and outboard dihedral angles in longitudinal and lateral-directional tests, small hinges were installed in the wing interface sections, as showed in Fig. 4.

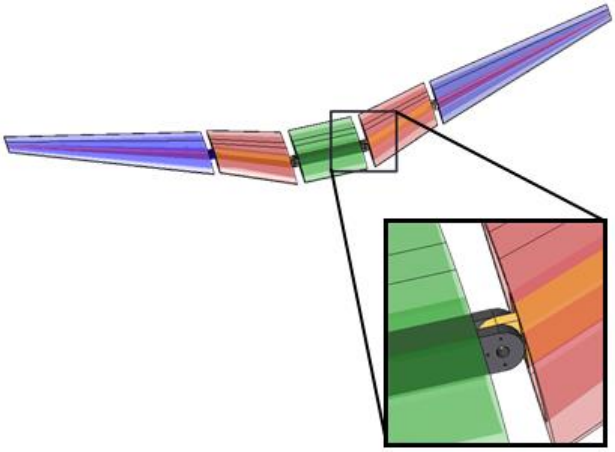

Fig. 4. Hinges used to modify dihedral angles

It can be observed from Fig. 4 that the wing was not constituted of a solid structure. In fact, it was built from ABS thermoplastic polymer using Rapid Prototyping Method as an external shell with two integrated spars. Additionally, one steel spar with hinges on the edges was added to each the wing section.

The external roughness of the wing after the Rapid Prototyping construction was not adequate for wind tunnel testing. It was necessary to sand all the external surfaces, apply sealant to smooth the imperfections and use automotive paint to properly configure the model to the experimental evaluation.

3 Results and Discussions

3.1 Uncertainty analysis

Uncertainty analysis for longitudinal coefficients was performed using the formulation proposed in reference [11]. The results are presented in Tab. 4.

Tab. 4. Uncertainty estimation for longitudinal coefficients

	C_L	C_D	C_m
Bias error	± 0.003	± 0.0009	± 0.0019
Precision error	± 0.001	± 0.0003	± 0.0005
Uncertainty [-]	± 0.004	± 0.0009	± 0.0019
Uncertainty [%]	± 1.4	± 1.4	± 1.3

The uncertainty [%] results presented in Tab. 4 are lower than 1.5% for all three longitudinal coefficients. These results are considered adequate to wind tunnel testing as they are within the limits established by Pope and Rae [12].

3.2 Lift coefficient

The lift coefficient results are presented from Fig. 5 to Fig. 7. In each figure the inboard dihedral was kept constant and the C_{L_α} derivative was plotted versus the variation of outboard dihedral.

From Fig. 5 to Fig. 7 it can be observed that the C_{L_α} slope decreases as the outboard dihedral angle is increased. This behavior is not noted in computational results from Tornado and XFLR5.

This change in C_{L_α} slope can be partially explained by the aspect ratio variation as the outboard dihedral is modified. In other words, there is a reduction of wing span and the project area towards lift direction.

Initially, however, it was believed that the variation of C_{L_α} slope would not be significant because the lift coefficient depends on the co-sine of dihedral angles, as stated by Purser and Campbell [13] for single dihedral wings, and this change was less than 1% when the outboard angle was increased from 2 degrees to 8 degrees during the experiment.

Nevertheless it can be noted from Fig. 5 to Fig. 7 a reduction of approximately 6% of C_{L_α} derivative when the outboard dihedral angle was modified from 2 degrees to 8 degrees.

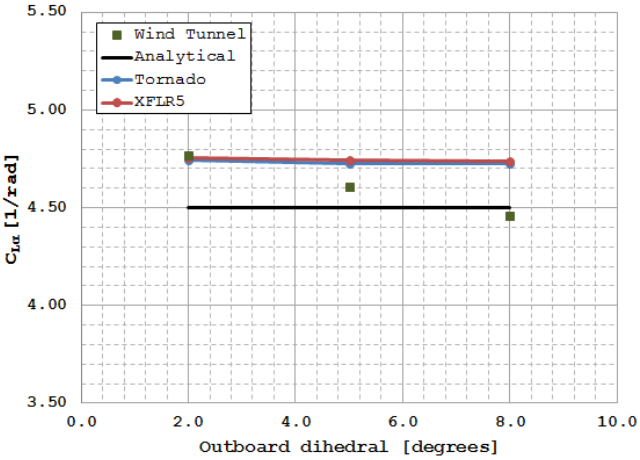

Fig. 5. C_{L_α} slope - inboard dihedral 5 degrees

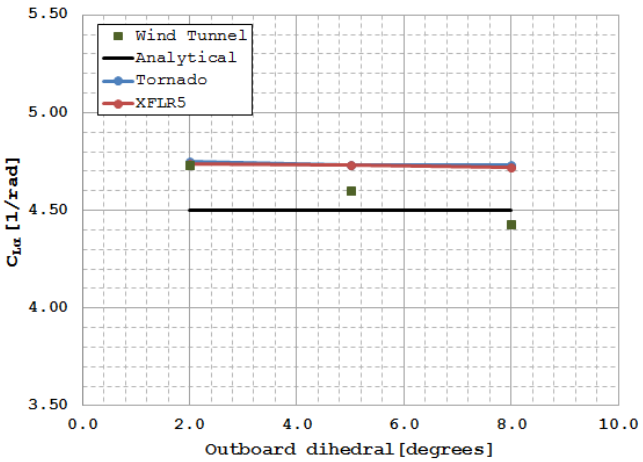

Fig. 6. C_{L_α} slope - inboard dihedral 8 degrees

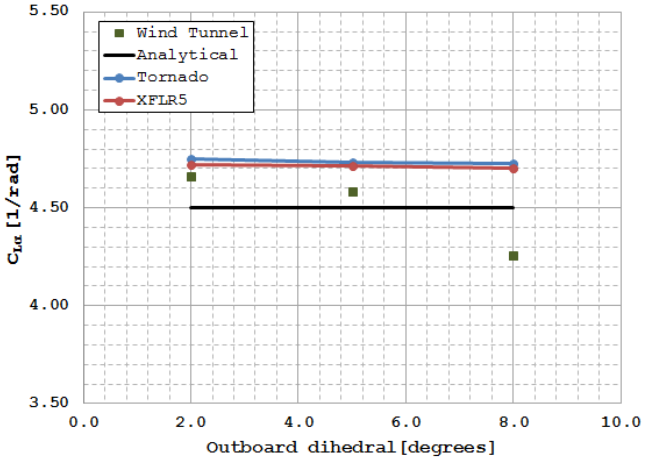

Fig. 7. C_{L_α} slope - inboard dihedral 11 degrees

3.3 Drag coefficient

The wind tunnel results for drag coefficients are presented from Fig. 8 to Fig. 10 as C_D versus C_L plots. Each figure is composed by three different curves, which represent the variation of outboard dihedral for a constant inboard dihedral.

It can be observed from Fig. 8 to Fig. 10 that the value of C_D for C_L equal to zero is similar for all configurations. This was expected as this parameter, the parasite drag, is mainly affected by the friction drag, and as the wetted areas of all the nine configurations tested are nearly the same, this component of total drag is not affected by the dihedral angles.

Additionally, from the C_D versus C_L plots, the Oswald efficiency factor (e) can be estimated using Eq. (6), according to reference [14]. The results for Oswald efficiency factor are presented in Tab. 5.

$$C_D = C_{D0} + \frac{C_L^2}{\pi A e} \qquad (6)$$

Tab. 5: Oswald efficiency factor (all dihedral values are in degrees)

Inboard dihedral	**Outboard dihedral**		
	2	**5**	**8**
5	0.92	0.88	0.87
8	0.90	0.86	0.85
11	0.88	0.85	0.84

From Tab. 5, it can stated that the Oswald efficiency factor depends on both dihedral angles. The Oswald factor decreases when the outboard dihedral angle is increased, for a constant inboard dihedral. And the Oswald factor decreases when the inboard dihedral is increased, for a constant outboard dihedral.

One possible explanation for this reduction of the Oswald factor, and consequently increase of drag coefficient, is related to the lift gradient along the wing span. For a fixed inboard dihedral and a given C_L, as the outboard dihedral angle increases, the difference between the lift generated by the two wing sections increases, and thus the intensity of vortex in this intersection enlarges. This hypothesis could be verified through the measurement of velocity field behind the gull wing, for instance, using hot wire anemometry.

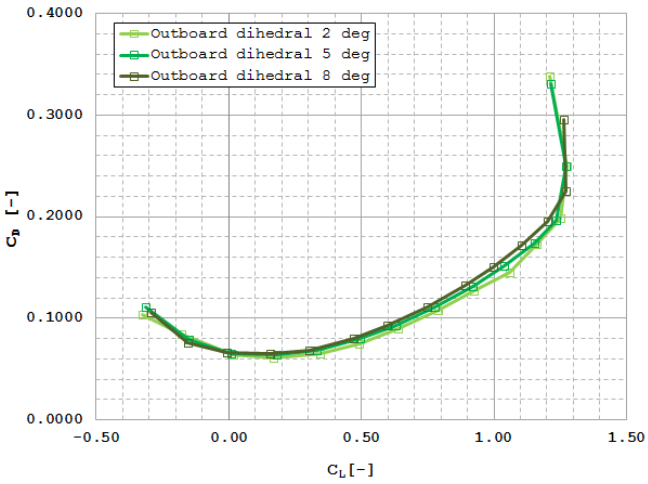

Fig. 8. C_D x C_L - inboard dihedral 5 degrees

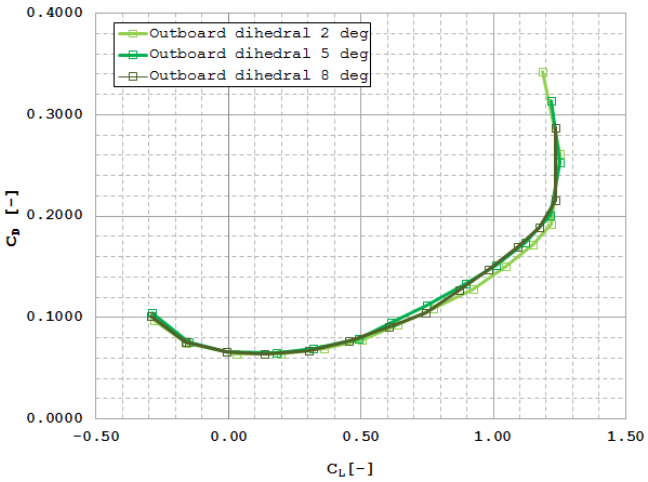

Fig. 9. C_D x C_L - inboard dihedral 8 degrees

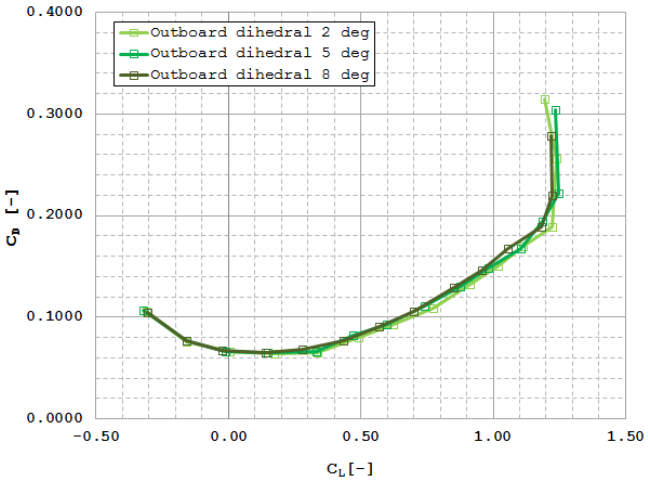

Fig. 10. C_D x C_L - inboard dihedral 11 degrees

3.4 Pitching moment coefficient

The pitching moment results are presented from Fig. 11 to Fig. 13. In these plots, comparisons of the dC_m/dC_L derivative obtained using the three types of analysis were done. Analytical results were obtained dividing Eq. (4) by Eq. (1).

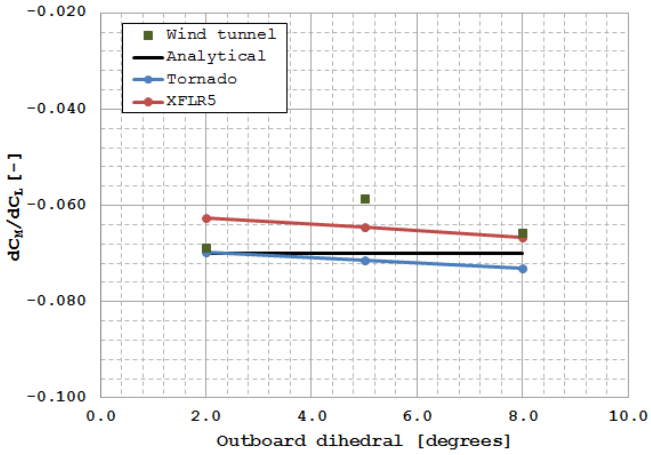

Fig. 11. dC_m/C_L - inboard dihedral 5 degrees

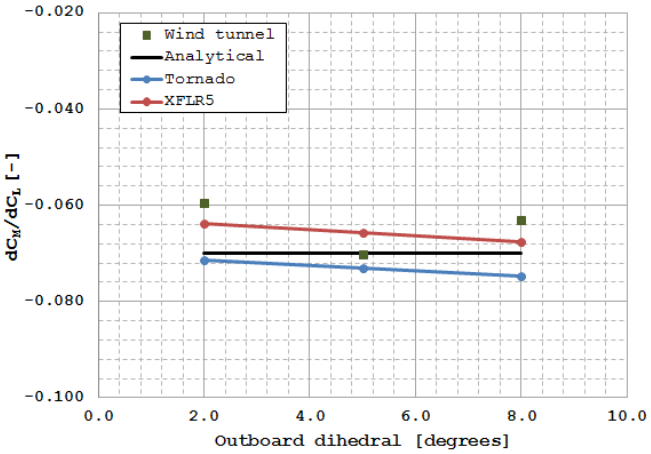

Fig. 12. dC_m/C_L - inboard dihedral 8 degrees

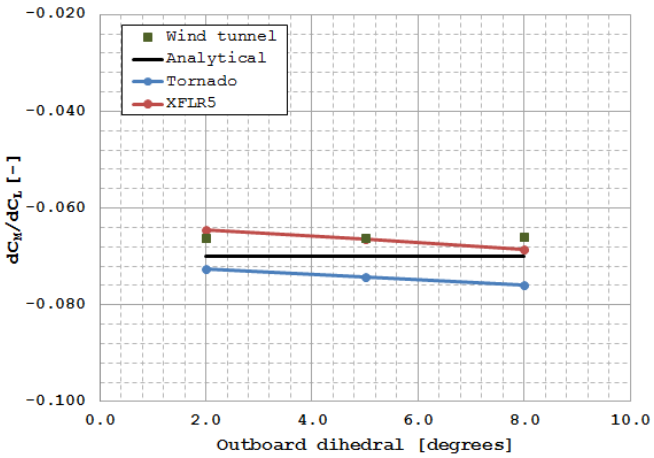

Fig. 13. dC_m/C_L - inboard dihedral 11 degrees

It can be noticed from the pitching moment curves that both computational tools, Tornado and XFLR5, indicate a reduction of dC_m/dC_L derivative of approximately 5% when the outboard dihedral angle was increased from 2 degrees to 8 degrees.

The wind tunnel results, however, show three different behaviors of dC_m/dC_L with the dihedral angles. In Fig. 11, the dC_m/dC_L derivative increases as the outboard dihedral was changed from 2 degrees to 5 degrees, and in the sequence it decreases when the outboard dihedral was modified from 5 degrees to 8 degrees. The exactly opposite behavior can be observer from Fig. 12. In addition, in Fig. 13 the dC_m/dC_L derivative is not affected when the outboard dihedral was augmented.

Taking these data into account, the wind tunnel results are inconclusive about the dependency of the pitching moment coefficient with the gull wing angles.

3.5 Yawing moment coefficient

To apply the Free Oscillation Method, it was necessary to induce a wing rotation, firstly with the wind tunnel switched off and secondly with it switched on. The model used in these tests is showed in Fig. 14.

Fig. 14. Wing model used for application of Free Oscillation Method

When there is no aerodynamics influence, both gull wing configuration tested – inboard 11 degrees / outboard 8 degrees and inboard 8 degrees / outboard 5 degrees (non-typical gull wing configurations were also tested and were

detailed in reference [8]) – presented similar damped oscillations, as can be noted in Fig. 15.

The "Non-dimensional amplitude" variable used in Fig. 15 and Fig. 16 was calculated as the yaw amplitude divided by the maximum yaw amplitude, achieved in the beginning of the test.

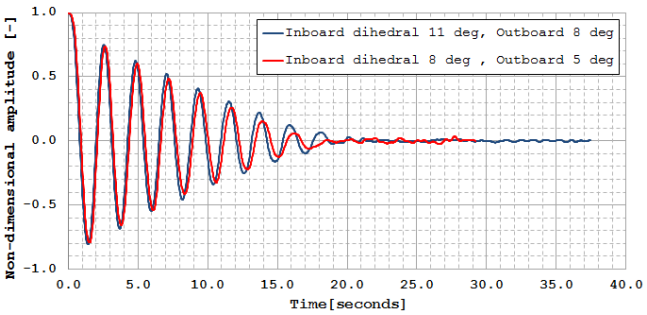

Fig. 15. Yawing oscillations – wind tunnel OFF

Although, when the airflow was accelerated up to 25 m/s, the configurations presented different responses. From Fig. 16, it can be observed that the oscillations were more damped for the configuration with larger dihedral angles.

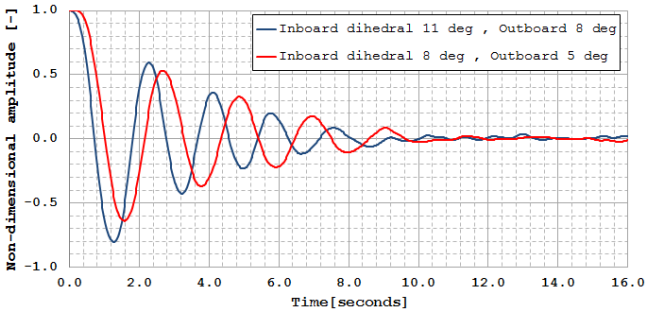

Fig. 16. Yawing oscillations – wind tunnel ON

Using wind tunnel data from Fig. 15 and Fig. 16, it was possible to calculate the yawing moment coefficient due to yaw rate derivative (C_{nr}) for the two configurations. The C_{nr} derivative was also calculated using Tornado, and the results are presented in Tab. 6.

Tab. 6: C_{nr} derivative results [1/rad]

Gull wing configuration	Wind tunnel	Tornado
Inboard 11 degrees Outboard 8 degrees	-0.004	-0.003
Inboard 8 degrees Outboard 5 degrees	-0.002	-0.002

From Tab. 6 one can affirm that the experimental and computational C_{nr} derivative results were similar.

Comparing data from Fig. 16 and Tab. 6, it can be stated that the C_{nr} derivative directly influences the oscillations' damping, and as more negative its value, more damped the oscillations.

4 Conclusions

In the present work, a bibliographic review about gull wings was performed, and a process intended to evaluate their characteristics was established. Initially, a reference wing geometry was defined, with several inboard and outboard dihedral combinations, and in the sequence three different methods of analysis, analytical computational and experimental, were used and their results were compared.

Wind tunnel results indicated that the gull wings have an influence on the lift and drag coefficients that are not forecasted by the analytical and computational methodologies. According to the wind tunnel results, the lift slope tends to decrease as the outboard dihedral angle is increased. With respect to the drag coefficient, it was noted that the Oswald efficiency factor decreases as the outboard angle is increased.

It was observed from computational results that the pitching moment coefficient to lift coefficient derivative decreases as the outboard wing dihedral increases. From experimental data, it was not possible to obtain the same conclusion.

The yawing moment wind tunnel results were in accordance with data from computational analysis. It was observed that when there is no aerodynamic influence, the oscillations are similar for both configurations tested, but when air flow is accelerated, the wing damping is directly proportional to the dihedral angles. From Fig. 16, it can be observed that the gull wing angles modify the frequency and amplitude of oscillations, and the inboard dihedral 11 degrees, outboard 8 degrees configuration suppresses the oscillation earlier.

5 References

[1] Roskam J. *Airplane design - part I: preliminary sizing of airplanes*. 2nd edition, DARcorporation, 2003.

[2] Ostrower J. A closer look at 787 wings flex. *Flight global*, May 30th, 2008. Available at http://www.flightglobal.com/blogs/flightblogger/2008/05/a_closer_look_at_787_wingflex.

[3] Pearson H A and Jones R T. Theoretical stability and control characteristics of wings with various amounts of taper and twist. *NACA Report 635*, Hampton, 1938.

[4] Ankenbruck H. Effects of tip dihedral on lateral-stability and control characteristics as determined by tests of a dynamic model in the Langley free flight tunnel. *NACA Technical Note 1059*, Washington 1946.

[5] Abdulharim M and Lind R. Flight testing and response characteristics of a variable gull-wing morphing aircraft. *AIAA Guidance, Navigation and Control Conference*. Providence, pp 1-16, 2004.

[6] Selig M S, Donovan J F and Fraser D B. *Airfoils at low speeds*. 1st edition, H. A. Stokely, 1989.

[7] Melin T. *A vortex lattice MATLAB implementation for linear aerodynamics wing application*. Master thesis – Department of Aeronautics, Royal Institute of Technology (KTH), Stockholm, 2000.

[8] Barbosa A A F. *Influence of gull wing on the aerodynamic coefficients of an airplane*. Master thesis – Engineering School of Sao Carlos, University of Sao Paulo, Sao Carlos, 2015.

[9] Engineering Science Data Unit (ESDU) 76028. *Lift-interference and blockage corrections for two-dimensional subsonic flow in ventilated and close wind tunnels*. The Royal Aeronautical Society, 1995.

[10] Ross J G and Lock R C. Wind-tunnel measurements of yawing moment due to yawing on a 1/5.5 scale model of the Meteor Mark F.III. *Aeronautical Research Council Reports and Memoranda*, London, 1952.

[11] Advisory Group for Aerospace Research and Development (AGARD). *Quality assessment for wind tunnel testing*. AGARD-AR-304. Specialized Printing Services Limited (SPS), 1994.

[12] Pope A and Raw W H. *Low speed wind tunnel testing*. 2nd edition, John Wiley & Sons, 1984.

[13] Purser P E and Campbell J P. Experimental verification of a simplified vee tail theory and analysis of available data on complete models with vee tails. *NACA ACR No L5AO3*, Langley, 1945.

[14] Raymer D P. *Aircraft design: a conceptual approach*. 2nd edition, American Institute of Aeronautics and Astronautics (AIAA), 1992.

6 Contact Author Email Address

Atila A. F. Barbosa: atila.barbosa@usp.br
Fernando M. Catalano: catalano@sc.usp.br

Copyright Statement